JOURNAL OF GEOPHYSICAL RESEARCH, VOL. 102, NO. D25, PAGES 29,867–29,880, DECEMBER 27, 1997

Near-field measurements on contrail properties from fuels with different sulfur content

A. Petzold,[1] R. Busen,[1] F. P. Schröder,[1] R. Baumann,[1] M. Kuhn,[1]
J. Ström,[2] D. E. Hagen,[3] P. D. Whitefield,[3] D. Baumgardner,[4]
F. Arnold,[5] S. Borrmann,[6] and U. Schumann[1]

Abstract. Microphysical properties of jet exhaust aerosol and contrails were studied in the near field of the emitting aircraft for different fuel sulfur contents. Measurements were performed behind two different aircraft (ATTAS test aircraft of type VFW 614 and Airbus A310-300) using fuels with sulfur contents of 6 ppm and 2700 ppm, respectively. At closest approach (plume age < 1 s), the total number concentrations exceeded the measuring range of the condensation particle counter, i.e., $N > 10^5$ cm^{-3}. The concentration of the dry accumulation mode aerosol, i.e., predominantly soot particles, was not affected by the fuel sulfur content. At a plume age of 10 s, an increase in total number concentration ($D_p > 0.01$ μm) by a factor of 3.5 in the high sulfur case compared to the low sulfur case was observed. The ultrafine condensation nuclei fraction (0.007 μm $< D_p < 0.018$ μm) contributed at maximum 70% to the total aerosol in the plume while this fraction was much less outside the plume. The high fuel sulfur content also caused an increase in the typical number concentrations of contrail particles by about one third with respect to low sulfur fuel, while the effective diameter of the size distribution was lowered at a fuel sulfur independent ice water content. The major differences in accumulation mode aerosol and microphysical contrail properties between the used aircraft were an increased number concentration of both the accumulation mode aerosol and the contrail particles in the Airbus A310-300 plume relative to the ATTAS plume. Part of the difference in contrail particles may be caused by different ambient conditions, but the major differences are assumed to be caused by different engine and wake properties.

1. Introduction

Engine exhaust products of high-flying jet aircraft are assumed to be an important source of new particles in the upper troposphere and the lower stratosphere [*Hofmann and Rosen*, 1978; *Arnold et al.*, 1992; *Fahey et al.*, 1995a, b; *Schumann et al.*, 1996]. As a direct consequence of the particle and water vapor emissions, the formation of visible contrails in the engine exhaust plume is observed under certain conditions which were explained first by *Schmidt* [1941] and *Appleman* [1953] and reexamined by *Schumann* [1996a]. To which extent contrails may perturb the chemical and radiative balance of the atmosphere is still an open question [*Schumann*, 1994; *Ponater et al.*, 1996]. Especially in consideration of higher particle concentration, smaller particle size and increased backscatter efficiency of a contrail compared to a natural cirrus [*Gayet et al.*, 1996a], the predicted growth of commercial air traffic requires a better understanding of air traffic impact on the atmosphere.

The distance behind the engines where contrails form and the microphysical properties of the contrails like contrail particle concentration, contrail particle size and optical thickness strongly depend on the ability of the emitted exhaust particles to act as cloud condensation nuclei (CCN) or ice nuclei. Based on balloon-borne measurements, *Hofmann and Rosen* [1978] suggested the subsequent oxidation of emitted SO_2 to gaseous sulfuric acid and binary nucleation of H_2SO_4-H_2O clusters as a possible mechanism for particle formation in an aircraft plume. Detailed model studies of the particle formation process [*Miake-Lye et al.*, 1994; *Kärcher et al.*, 1995, 1996a; *Zhao and Turco*, 1995; *Brown et al.*, 1996a] indicated the formation of sub-nanometer H_2SO_4-H_2O clusters (0.6 - 1.2 nm in diameter) via homogeneous nucleation within the young exhaust plume (age < 1 s). The first laboratory experimental indications of the existence of the H_2SO_4-H_2O clusters in a jet engine exhaust plume were given by *Frenzel and Arnold* [1994]. Calculated nucleation rates vary between 10^9 cm^{-3} s^{-1} and 10^{11} cm^{-3} s^{-1} for average to high fuel sulfur levels. In these cases gaseous H_2SO_4 is assumed to be almost completely depleted via homogeneous nucleation after a plume aging time of 1-2 s, i.e., within a distance of 200 m

[1] Deutsches Zentrum für Luft- und Raumfahrt (DLR), Institut für Physik der Atmosphäre, Oberpfaffenhofen, Germany.
[2] Department of Meteorology, Stockholm University, Stockholm, Sweden.
[3] Cloud and Aerosol Science Laboratory, University of Missouri-Rolla.
[4] National Center for Atmospheric Research, Boulder, Colorado.
[5] Atmospheric Physics Division, Max-Planck-Institut für Kernphysik, Heidelberg, Germany.
[6] Institut für Physik der Atmosphäre, Johannes Gutenberg Universität, Mainz, Germany.

Paper number 97JD02209.
0148-0227/97/97JD-02209$09.00

from the engine exit [*Kärcher et al.*, 1995, 1996a]. The values given for the conversion rate of SO_2 into H_2SO_4 in the near field exhaust (plume age < 2 s) are between 0.5% [*Kärcher et al.*, 1995] and 2% [*Brown et al.*, 1996a]. *Brown et al.* [1996b] pointed out recently, as was known for conventional gas turbines [e.g., *Farago*, 1991], that the main conversion product of fuel sulfur besides SO_2 at the engine exit is SO_3 in addition to gaseous sulfuric acid. The fuel sulfur to S(VI) conversion ratio may vary with fuel sulfur content. The authors calculate a conversion ratio from less than 1% to more than 4% for fuel sulfur contents of 5400 ppm and 2 ppm, respectively.

Kärcher et al. [1995] showed that exclusive growth of H_2SO_4-H_2O clusters via water uptake, coagulation, and subsequent homogeneous freezing cannot account for sufficient ice particle production in a plume just below liquid water saturation. Only the activation of exhaust soot particles by agglomeration with H_2SO_4-H_2O droplets followed by heterogeneous freezing of the mixed aerosol could serve as an efficient source for activated condensation nuclei at threshold formation conditions [*Schumann et al.*, 1996; *Kärcher et al.*, 1996a, b; *Brown et al.*, 1996a]. In the initial stage of contrail formation, homogeneous freezing time scales for H_2SO_4-H_2O droplets at the same distance can be longer than the respective time scales for heterogeneous freezing of H_2SO_4-H_2O-covered soot particles [*Kärcher et al.*, 1996b]. Heterogeneous freezing is therefore assumed to start somewhat earlier than homogeneous freezing.

At temperatures above 220 K almost all ice particles are assumed to contain soot inclusions typically smaller than 0.5 μm in diameter [*Kärcher*, 1996]. These model predictions are supported by samples of cloud element residues in contrails with a counterflow virtual impactor which show that almost all residue particles in a contrail are smaller than 0.5 μm in diameter and consist of black carbon [*Ström*, 1996; *Petzold et al.*, 1997].

Summarizing the present knowledge on the formation of visible contrails, this process requires at first the saturation with respect to water inside the plume. The fuel sulfur content gives rise to the formation of gaseous H_2SO_4 which nucleates homogeneously to sub-nm H_2SO_4-H_2O clusters in the near field plume. The formation of ice particles starts with the soot-induced condensation and heterogeneous freezing, followed by homogeneous freezing of the largest purely volatile particles. These contrail particles grow rapidly by water uptake and form a visible contrail when they initiate in the liquid phase and then freeze [*Schumann*, 1996b].

Up to now only few in-situ measurements of microphysical and chemical properties of contrails have been presented [*Knollenberg*, 1972; *Baumgardner and Cooper*, 1994; *Fahey et al.*, 1995a, b; *Busen and Schumann*, 1995; *Pitchford et al.*, 1991; *Schumann et al.*, 1996; *Gayet et al.*, 1996a; *Hagen et al.*, 1996]. The studies by *Knollenberg* [1972] and *Gayet et al.* [1996a] focused on the properties of persisting contrails. Measurements in the exhaust plume of the Concorde [*Fahey et al.*, 1995a] and the ER-2 [*Fahey et al.*, 1995b] at plume ages of more than 10 min gave evidence for enhanced condensation nuclei (CN) concentrations of 6×10^7 (standard cm)$^{-3}$ (Concorde) and 2×10^6 (standard cm)$^{-3}$ (ER-2) during plume encounters. The ratio of nonvolatile to volatile particles varied between 0.5 and 0.1, i.e., the major fraction of emitted particles with diameters larger than 0.009 μm consisted of volatile material, assumed to be sulfuric acid with water, but not of soot. From these findings the authors estimated a S to H_2SO_4 conversion rate of at least 12 to 45% [*Fahey et al.*, 1995a] which is different from the model results and first experimental results given above. Ice crystals were not present during these campaigns.

Ground-based studies by *Petzold and Schröder* [1997] in the exhaust of the ATTAS jet engine indicated a bimodal soot number distribution with the primary soot mode at 0.045 μm diameter and an agglomeration mode at 0.18 μm diameter. The contrail study by *Hagen et al.* [1996] at a distance of 8 km behind the aircraft reported also a distinct aerosol mode in the size range of 0.1 μm < D_p < 0.2 μm.

Pitchford et al. [1991] measured the hygroscopic behavior of jet exhaust aerosol at a distance of 200 m behind a Sabreliner at an altitude of 800 m and ambient temperature of 284.5 K. They observed CN concentrations of 3×10^5 cm^{-3} and CCN concentrations of 300 cm^{-3}, yielding an activated exhaust aerosol fraction of about 0.001 at 0.8% supersaturation. The first but preliminary near-field contrail study with respect to the size distribution of contrail particles was reported by *Baumgardner and Cooper* [1994]. They measured with a forward scattering spectrometer probe FSSP-300 in the wake of a Lear jet 35 at distances from 150 m up to 1.5 km. CN concentrations increased up to 7000 cm^{-3}; the mean diameter of ice crystals was 1.5 μm.

Recently, experiments named SULFUR 1 to SULFUR 3 concerning the influence of the fuel sulfur content on contrail forming properties of the exhaust aerosol were performed using the twin-engine ATTAS test aircraft of type VFW-614 of the Deutsches Zentrum für Luft- und Raumfahrt (DLR) which was operated with different sulfur-containing fuels [*Busen and Schumann*, 1995; *Schumann et al.*, 1996]. The fuel sulfur contents were set to 2 and 250 ppm [*Busen and Schumann*, 1995] and to 170 and 5500 ppm [*Schumann et al.*, 1996]. In the first experiment no visible difference in the onset of contrail formation was observed between the low sulfur fuel and the medium sulfur fuel. In the second experiment the higher sulfur emissions caused a larger optical thickness of the contrail, which showed a slightly brown color. This color effect could be related to the higher concentration and the smaller size of the contrail particles in the high sulfur case [*Schumann et al.*, 1996; *Gierens and Schumann*, 1996]. Moreover, these experiments show that sulfur emissions have little impact on the threshold conditions for contrail formation. On the other hand, these measurements provided first experimental evidence that higher fuel sulfur content results in about 25% higher concentrations of CN with D_p > 0.007 μm and about 50% higher fraction of activated soot particles with D_p > 0.018 μm.

Objectives of the experiment SULFUR 4 presented here were the effects of varying fuel sulfur content on microphysical parameters, number concentration and size distribution of the exhaust aerosol, number concentration and size distribution of particles inside the formed contrail, and the concentration of gaseous sulfuric acid at very young plume ages of 1-2 s. An overview on the experimental flights including first results with respect to condensation particles, dry accumulation mode aerosol and contrail properties will be presented in the following.

2. Experimental Details

During the SULFUR 4 experiment performed on March 12, 13 and 15, 1996, over southern Germany, contrails were generated either by the DLR test aircraft ATTAS (as in the previous studies SULFUR 1 to SULFUR 3 [*Schumann et al.*, 1996]) or by a commercial aircraft AIRBUS A310-300 of Lufthansa AG using fuel with different sulfur contents. Both are twin-engine subsonic jet aircraft but of different size (wing spans 21.5 m and 43.9 m), age (built 1971 and 1991) and engines (Rolls-Royce/SNECMA M45H Mk501 and GE CF6-80 C2A2). The near-field observations were conducted by the Falcon research aircraft of DLR, which followed both aircraft at distances of between less than 100 m and 4 km (see Plates 1 to 3). The findings reported here are based on observations where sequences of burning fuel with either low or high sulfur content have been optimized in temporal and spatial extent in order to keep the influences of changing environmental conditions at a minimum. The distances between contrail-generating aircraft and measuring aircraft were deduced from both Falcon cockpit video recordings and GPS satellite positioning recordings on the Falcon and ATTAS. The high sulfur content of 3000 ppm was achieved by adding exact amounts of dibutylsulfide to the fuel [*Busen et al.*, 1996]; the lower sulfur contents were < 6 ppm (ATTAS) and 850 ppm (AIRBUS A310-300). It should be noted that the Airbus flew at the lowest possible speed of 180 m s^{-1} to allow the Falcon to follow within the wake.

The Falcon was equipped with standard meteorological instrumentation to measure static air temperature T, static pressure p, humidity based on Vaisala- and Lyman-α-hygroscopy and three-dimensional wind components [*Schumann et al.*, 1996]. Particle microphysics was characterized with (1) a passive cavity aerosol spectrometer probe PCASP-100X (PMS Inc.) to measure the dry accumulation mode aerosol (nominal size range 0.1 μm < D_p < 3.0 μm), (2) a FSSP-300 (PMS Inc.) for in-situ classification of the contrail particles (size range 0.3 μm < D_p < 20 μm [*Strapp et al.*, 1992]), (3) a prototype multi-angle aerosol spectrometer probe (MASP) for simultaneous measurements of particle forward/backward scattering (size range 0.4 μm to 10 μm [*Baumgardner et al.*, 1996]), and (4) the Mobile Aerosol Sampling System (MASS; University of Missouri-Rolla) based on aerosol classification by electrical mobility and subsequent detection by condensation particle counters (CPC). The MASS was used to characterize the size distribution in the size range from 0.01 μm to 0.4 μm [*Hagen et al.*, 1996]. This system requires aerosol sampling in a holding tank and allows only few integrated size distribution measurements during one flight. An interstitial aerosol inlet [*Schröder and Ström*, 1997] connected to three CPCs (modified TSI 3760/3010) with lower cutoff diameters of 0.007 μm (N_7), 0.01 μm (N_{10}) and 0.018 μm (N_{18}) was used to achieve number concentrations of the aerosol with D_p > 0.01 μm (N_{10}) and the ultrafine condensation nuclei mode (UCN: 0.007 μm < D_p < 0.018 μm) aerosol, which corresponds due to its lower and upper size limits to the very young condensation nuclei and can be taken as an indicator for the formation of new particles. The aircraft-based ion mass spectrometers (IOMAS; Max-Planck-Institut für Kernphysik) were used for the measurement of gaseous H_2SO_4 and ions (F. Arnold et al., Gaseous ion composition measurements in the young exhaust plume of a jet aircraft at cruising altitudes: Implications for aerosols, gaseous sulfuric acid and its homogeneous nucleation, submitted to *Geophysical Research Letters*, 1997; hereinafter referred to as submitted paper). The detection limit for gaseous H_2SO_4 is 6×10^6 molecules cm^{-3}. A summary of the complete instrumentation is given in Table 1, further details are given in Appendix A.

The measurements behind both the ATTAS and A310-300 were performed mainly at two distances of < 250 m (short distance, plume age < 2 s) and 1800 m (medium distance, plume age ≈ 10 s). Additionally, measurements at about 100 m distance behind the leading aircraft with and without visible contrails were realized after extensive theoretical studies on flow field induced turbulence behind an aircraft [*Gerz and Ehret*, 1997]. All measurement flights were bound to the upper troposphere and the tropopause region with ambient air temperatures of 215 K to 230 K.

Flight conditions and fuel sulfur contents during the experiment are summarized in Table 2. Corresponding to the strong differences in relative humidity, the aircraft generated dense contrails on March 13 and March 15, while on March 12 a barely visible plume was present, consistent with the Schmidt-Appleman criterion [*Schumann*, 1996a] (see Table 2). The data analyses will focus on flight sequences under contrail forming conditions.

3. Results and Discussion

3.1. ATTAS Plume Properties

To describe meteorological conditions and general aerosol properties inside the plume, the plume data of interest are temperature excess ΔT with respect to ambient air, water vapor mixing ratio r, and particle concentration N_{10}. The maximum values at closest approach are listed in Table 3 for all flights. The particle number concentrations N_{10} are given only as a lower limit because the CPCs were operated close to the upper detection limits at flight distances < 400 m. It is very likely that the real number concentration values exceeded 10^5 cm^{-3} and that possible differences between the low and high sulfur fuel cases could not be resolved at such close flight distances. Temperature excess ΔT and water vapor mixing ratio r are distinct functions of the plume age or measuring distance, respectively. The measured excess values can be used to determine plume dilution (U. Schumann et al., Dilution of aircraft exhaust plumes at cruise altitudes, submitted to *Atmospheric Environment*, 1997; hereinafter referred to as submitted paper) and are roughly consistent with estimated plume dilution values and corresponding models [e.g., *Zhao and Turco*, 1995]. More details on physical properties of a jet exhaust plume at very short distances behind the emitting aircraft will be the subject of a future publication.

In Figure 1 flight distance d, static air temperature T, water vapor mixing ratio r, and vertical component w of the air motion are given for a short segment of the March 12 flight behind the ATTAS, where the closest approach of 80 m during the whole experiment was realized (see Plate 2). During this period, three plume measurements were taken at flight level 310 with different fuels being burned. The first

Plate 1. Photo of the Falcon showing the positions of the aerosol spectrometers (wing stations) and the sampling inlet on the roof of the aircraft.

Plate 2. Photo of the ATTAS from the Falcon cockpit at flight distance $d < 200$ m (FL 310 on March 12, 1996).

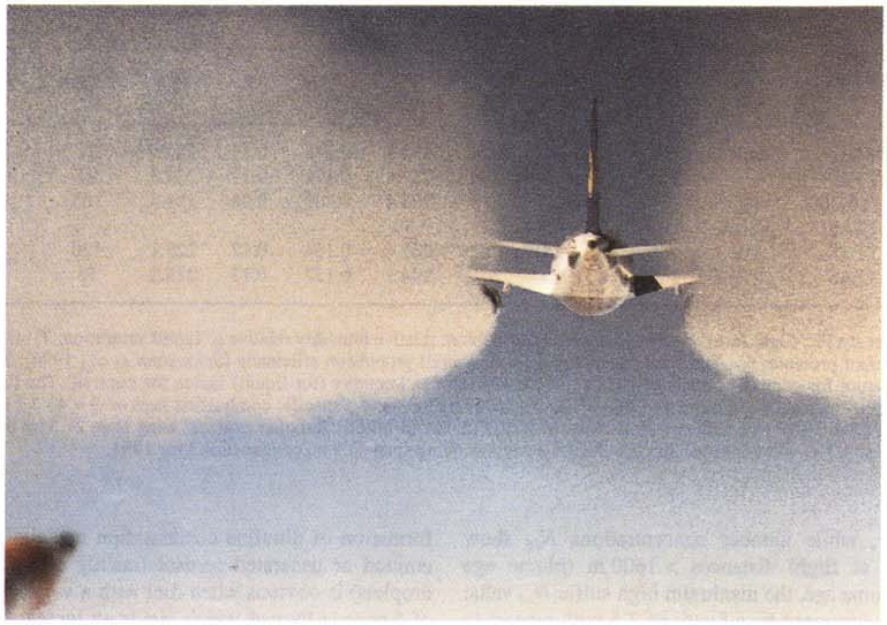

Plate 3. Photo of the Airbus A310-300 from the Falcon cockpit at flight distance $d < 400$ m (FL 350 on March 13, 1996).

attempt started with the first dip in the w plot, but the Falcon did not stay in the exhaust plume from the beginning, as there is no distinct signal in temperature or humidity. Later on, the successful positioning of the Falcon can be seen in the temperature increase of up to 11 K and the humidity increasing by about a factor of 10. In the vertical wind component w a downward air motion of more than 10 m s^{-1} is documented (as the data in Figure 1 are smoothed to 1 Hz resolution, small-scale fluctuations with even larger w of up to -14 m s^{-1} are not visible).

Figures 2a and 2b show the time series of number concentration N_{10} and flight distance d in the near field of the plume (2a) and at medium flight distance (2b) as a function of decimal time for the ATTAS flight on March 15 at FL 310. During sequences 12.64 to 12.72 (Figure 2a) and 12.98 to 13.06 (Figure 2b) fuel with a sulfur content of 2700 ppm was burned on both engines, while sequences 12.77 to 12.82 (Figure 2a) and 12.84 to 12.91 (Figure 2b) correspond to the low sulfur fuel case (fuel content 6 ppm for both engines). It can be clearly seen that the Falcon succeeded in staying inside the plume for several minutes in each case. The variations in peak height are due to small-scale movements of the Falcon across the ATTAS plume cross section in order to bring the different inlets and sensors into their optimum sampling positions.

The number concentration N_{10} is plotted as a function of flight distance d in Figures 3a and 3b corresponding to the sequences shown in Figs. 2a and 2b as time series. An effect of fuel sulfur content on the particle formation could not be resolved in the near field ($d < 300$ m, plume age ≤ 2 s) as

Table 1. Falcon Instrumentation

	Instrument	Measuring Range	Research Facility
Meteorological parameters	T, p, RH, water vapor mixing ratio r, vertical wind component w		DLR [*Schumann et al.*, 1996]
Particle microphysics	PCASP-100X	0.1 μm < D_p < 3.0 μm	Universität München
	FSSP-300	0.3 μm < D_p < 20 μm	Universität Mainz
	MASP	0.4 μm < D_p < 10 μm	NCAR/RAF [*Baumgardner et al.*, 1996]
	Mobile Aerosol Sampling System (MASS)	0.01 μm < D_p < 0.4 μm	University of Missouri-Rolla [*Hagen et al.*, 1996]
	Interstitial aerosol inlet with 3 CPCs (cutoff: 0.007 μm, 0.01 μm, 0.018 μm)	0.007 μm < $D_p \leq$ 1.0 μm	Stockholm University [*Schröder and Ström*, 1997]
Gas phase	Aircraft-based Ion Mass Spectrometers (IOMAS) for the measurements of gaseous H_2SO_4 and ions	Detection limit for H_2SO_4: 6×10^6 molecules cm^{-3}	Max-Planck-Institut für Kernphysik, Heidelberg [*F. Arnold et al.*, submitted manuscript, 1997]

Table 2. Measurement Flights During SULFUR 4: Flight Conditions, Engine Parameters, and Fuel Sulfur Contents

Date	Aircraft	FL, hft	V, m s^{-1}	RH, %	T, K	p, hPa	m_F, kg s^{-1}	η	T_{LC}, K	RH_{max}, %	Sulfur content, ppm
March,12	ATTAS	240	160	10 ± 10	234	392.7	0.176	0.17	224.9	11	6, 2830
March 12	ATTAS	310	175	20 ± 10	230	287.4	0.170	0.17	222.3	27	6, 2830
March 13	A310-300	350	180	15 ± 10	215	238.4	0.400	0.28	221.6	165	850, 2700
March 14	ATTAS	ground	0	22 ± 10	281	950					6, 2830
March 15	ATTAS	310	165	40 ± 15	221	287.4	0.164	0.17	223.1	120	6, 2700
March 15	ATTAS	270	160	45 ± 15	231	344.3	0.157	0.17	225.2	55	6, 2700

Abbreviations are FL, flight level; V, true air speed; RH, ambient relative humidity relative to liquid saturation; T, static air temperature; p, ambient pressure; m_F, fuel flow rate per engine; η, overall propulsion efficiency [*Schumann et al.*, 1996]; T_{LC}, critical ambient temperature for contrail formation; RH_{max}, maximum relative humidity (for liquid) inside the contrail. The fuel analysis resulted in a water vapor emission index of $EI_{H2O} = 1.230 \pm 0.009$ kg kg^{-1}, and a specific combustion heat of $Q = 43.3 \pm 0.1$ MJ kg^{-1} for all cases. ATTAS: VFW 614 with two Rolls-Royce/SNECMA M45H Mk501 turbofan engines; wing span 21.5 m; construction year 1971. Airbus: A310-300 with two GE CF6-80C2A2 engines; wing span 43.9 m, construction year 1991.

mentioned above, while number concentrations N_{10} show large differences at flight distances > 1600 m (plume age ≈ 10 s). At this plume age, the maximum high sulfur N_{10} value (3.5×10^4 cm^{-3}) is increased by a factor of 3.5 with respect to the maximum low sulfur N_{10} value (1.0×10^4 cm^{-3}). Almost the same enhancement factor holds for the average N_{10} values, as can be seen in Table 4.

In Figure 4 the UCN fraction of the total aerosol is plotted as a function of decimal time in combination with the number concentration of particles larger than 0.01 μm for the ATTAS medium flight distance case. These observations give evidence of a strong correlation between jet exhaust components and a significant increase in the UCN concentration. Outside the plume the UCN fraction is much weaker than inside the plume, where this fraction by far exceeds 30% with a maximum UCN fraction of more than 70%. The sensitivity of the UCN fraction measurement to jet exhaust aerosol is demonstrated during the weak plume encounter around time 12.95 (Figure 4). There is only a slight enhancement of the number concentration but a strong increase in the UCN fraction. The average and maximum UCN fractions as well as average and maximum N_{10} values are summarized in Table 4 for the medium flight distance case including background aerosol values obtained from flight segments between plume encounters.

In conclusion, the above results can be summarized as follows: at the plume age of ≈ 10 s, the CPC measurements indicate a clear influence of fuel sulfur content on the formation of ultrafine condensation nuclei. The effect of the emitted or generated aerosol (mainly soot and sulfuric acid droplets) is obvious when fuel with a very low sulfur content of 6 ppm is burned which yields an increase of the number concentration by a factor of 25 inside the plume with respect to the undisturbed background aerosol. In contrast, the increase in the fuel sulfur content from 6 ppm to 2700 ppm results in an additional enhancement of the N_{10} concentration by a factor of 3.5, indicating evidence for fuel sulfur impact on the particle formation in the aircraft exhaust. Part of this rather small increase may be explained by model results, which show a decrease in fuel sulfur conversion to S(VI) from more than 5% in the low sulfur fuel case to about 2% at a fuel content of 2700 ppm [*Brown et al.*, 1996b].

3.2. ATTAS Contrail Properties

The microphysical properties of the contrails are summarized in Table 5 for the different measuring conditions with respect to the accumulation mode aerosol and the contrail particles. Respective size distributions are plotted in Figures 5a - 5d for the ATTAS flight on March 15 at FL. 310, including the measurements of the condensation nuclei (N_{10}) with the CPC. Detailed information on the analysis of the size distributions is given in Appendix B.

At the short measuring distance (Figures 5a and 5b) two different cases can be distinguished: the contrail particle size distributions with an excess temperature $\Delta T > 1.5$ K are

Table 3. Maximum Plume Parameters Temperature Excess ΔT_{max}, Water Vapor Mixing Ratio r, and Number Concentration N_{10} ($D_p > 0.01$ μm) With Respect to Ambient Conditions p and T at Closest Approach *

Date	Aircraft	Minimum Distance, m	ΔT_{max}, K	r, g kg^{-1}	N_{10}, cm^{-3}
March 12 (FL 310)	ATTAS	80	11	0.46	$> 5 \times 10^4$
March 13	A310-300	100	2.8	0.11	$> 5 \times 10^4$
March 14 (ground)	ATTAS	1.5	- - -	- - -	$0.18 - 1.5 \times 10^7$
March 15 (FL 310)	ATTAS	100	6.8	0.30	$> 8 \times 10^4$

* The estimated N_{10} ground test values (March 14) are added for comparison [*Petzold and Schröder*, 1997].

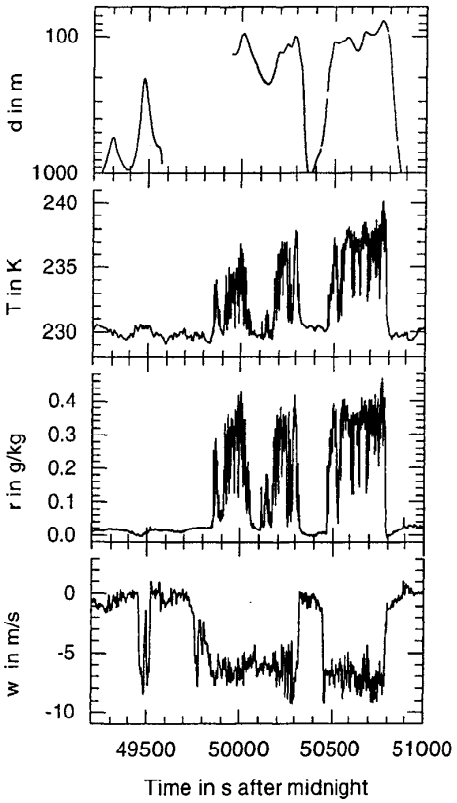

Figure 1. Flight distance d, static air temperature T, water vapor mixing ratio r, and vertical wind component w in the wake of the ATTAS in dry air (FL 310 on March 12, 1996); no visible contrail was formed.

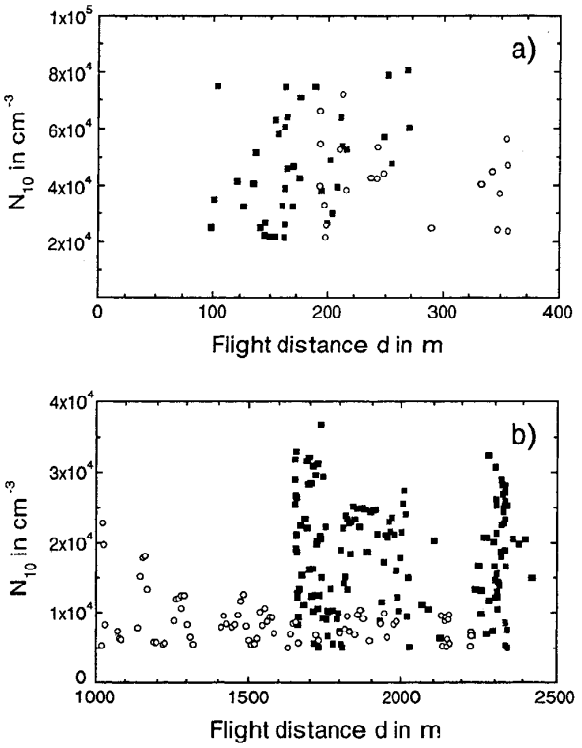

Figure 3. Number concentration N_{10} as a function of flight distance d (a) in the near field of the ATTAS and (b) at medium flight distance at flight level 310 on March 15, 1996, for both high (squares) and low (circles) fuel sulfur content.

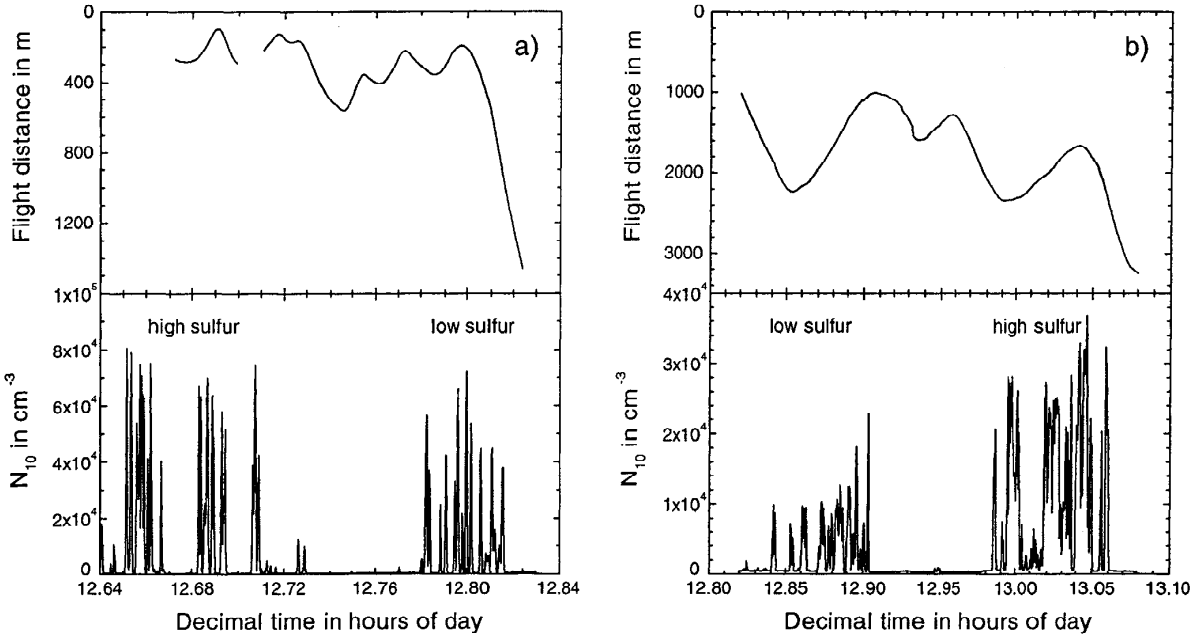

Figure 2. Number concentration N_{10} ($D_p > 0.01$ μm) and flight distance d in the wake of the ATTAS at flight level 310 on March 15, 1996; Figures 2a and 2b correspond to short and medium flight distances, respectively.

Table 4. Number Concentration N_{10} and Ultrafine Condensation Nuclei Fraction (UCN: 0.007 μm < D_p < 0.018 μm) of the Total Aerosol at a Measuring Distance of 1800 m (Plume Age ≈ 10 s) Inside the ATTAS Plume (FL 310 on March 15, 1996)

	Flight Distance 1800 m; Plume Age 10 s*	
	Mean	Maximum
Background		
N_{10}, cm^{-3}	300 ± 50	380
UCN, %	7 ± 4	19
Low sulfur		
N_{10}, cm^{-3}	7.5 ± 0.2 × 10^3	1.0 × 10^4
UCN, %	31 ± 13	77
High sulfur		
N_{10}, cm^{-3}	2.1 ± 0.4 × 10^4	3.5 × 10^4
UCN, %	43 ± 13	78

* Analyzed peaks with height N > 2000 cm^{-3}.

interpreted as measurements inside the center of the plume, while the size distributions with ΔT < 0.15 K are related to measurements at the more diluted plume edge, where evaporation of the contrail particles becomes important. This interpretation is straightforward because the Falcon stayed at a constant measuring distance while moving slightly across the plume perpendicular to the flight direction. At the medium measuring distance (Figures 5c and 5d) the distinct differences in the contrail particle size distributions have vanished because it was much easier to position the Falcon inside the formed contrail due to the increased plume cross section.

The number concentration of contrail particles N_{cp} shows no dependence on the fuel sulfur content at the young plume age of < 2 s (Figures 5a and 5b). An obvious difference occurs in the ice water content which is increased by a factor of 3 in the case of the low sulfur fuel contrail with respect to the high sulfur fuel contrail. Also the mean diameter and the effective diameter of the ice crystals are smaller in the high sulfur fuel case. The latter is consistent with the visible differences between contrails from low and high sulfur fuel, as reported by *Schumann et al.* [1996]. However, there is no explanation for the observed discrepancy in the ice water content between the low sulfur and the high sulfur case because the amount of condensable water depends on the emitted water vapor and is therefore not affected by the fuel sulfur content. One reason for the observed deviations may be due to the highly turbulent and inhomogeneous conditions inside the plume at an age < 2 s and the small plume cross section compared to the dimensions of the measuring aircraft, which allows only random sampling of the contrail particles. For this reason, these size distributions should be viewed as a transient state in the evolution of a contrail.

In the aged state after 10 s (Figures 5c and 5d), when the evolution of the contrail has slowed down, the higher fuel sulfur content results in an increase in N_{cp} by about one third, while the ice water content is almost the same for both contrails. Thus the data from the longer measuring distance seem to describe a more stable state in contrail history. It should be noted that besides the ice water content of about 2 mg m^{-3}, the specific surface of about 2000 μm^2 cm^{-3} is not affected to a major extent by the fuel sulfur content.

In summary, the above presented features of no significant difference in contrail particle number concentration N_{cp} at a plume age < 2 s and an increased N_{cp} value in the high sulfur fuel case with respect to the low sulfur fuel case at a plume age of about 10 s follow the model predictions [e.g., *Kärcher*, 1996; *Kärcher et al.*, 1996b]. Thus the data suggest that at a plume age of < 2 s the number concentration of contrail particles is controlled by the number concentration of emitted soot particles which is independent from fuel sulfur content [*Petzold and Schröder*, 1997]. At a plume age of 10 s, the higher fuel sulfur content yields an increased contrail particle number concentration which may be due to homogeneous freezing of H_2SO_4-H_2O droplets. Details of this outlined picture depend on the relative timescales for heterogeneous freezing of activated soot particles and homogeneous freezing of H_2SO_4-H_2O droplets [*Kärcher et al.*, 1996b].

In the near field behind the contrail-generating aircraft, the accumulation mode aerosol, which can be viewed as the soot particles emitted from the engine, shows no significant difference between the low sulfur and the high sulfur fuel case neither in number concentration nor in the slope k of the size distribution. According to scavenging processes with respect to the smaller exhaust aerosol particles, the slope of the size distribution and the number concentration are decreasing with increasing contrail age. The same behavior is deduced from the slope k of the size distributions measured with the MASS [*Busen et al.*, 1996]. As can be seen also from the data in Table 5, the Junge approximation is reasonable for the accumulation mode aerosol because in all cases the correlation is of statistical significance at a 99% level (n = 6 data points).

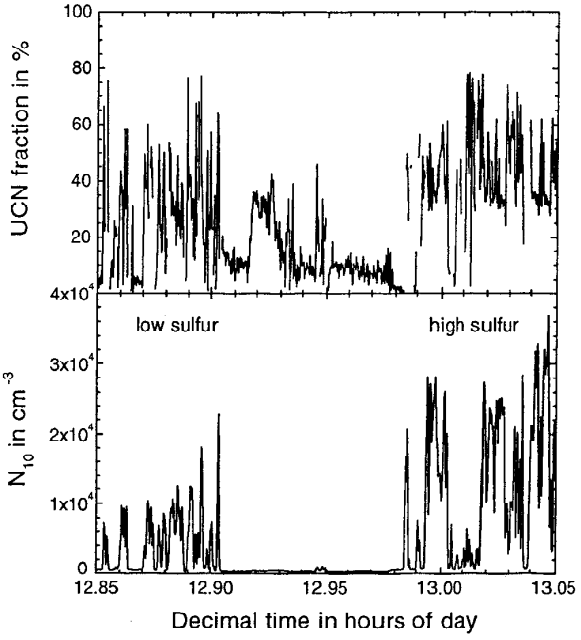

Figure 4. Number concentration N_{10} and ultrafine condensation nuclei fraction (UCN: 0.007 μm < D_p < 0.018 μm) of the total aerosol in the wake of the ATTAS at flight distances from 1 km to 2.6 km for fuel with low sulfur and high sulfur content (FL 310 on March 15, 1996).

Table 5. Microphysical Parameters of Accumulation Mode Aerosol and Contrail Particles

	Flight Distance 250 m; Plume Age < 2 s				Flight Distance 1800 m; plume age ≈ 10 s	
	Plume Center		Plume Edge			
	Sulfur Content		Sulfur Content		Sulfur Content	
Parameter	6 ppm	2700 ppm	6 ppm	2700 ppm	6 ppm	2700 ppm
Excess temperature ΔT, K	> 1.5	> 1.5	< 0.15	< 0.15	0	0
Accumulation mode aerosol *						
N, cm^{-3}	3850 ± 560	3600 ± 1180			1230 ±390	730 ± 170
k	- 4.6	- 4.7			- 3.9	- 4.1
r^2	0.96	0.98			0.96	0.97
Contrail particles +						
N_{cp}, cm^{-3}	860	750	690 ± 70	1060 ± 250	1490 ± 180	2000 ± 200
DM, µm	2.67	1.86	1.50	0.90	1.20 ± 0.06	1.07 ± 0.05
D_e, µm	3.46	2.34	2.34	1.36	1.74 ± 0.06	1.48 ± 0.04
c_A, µm^2 cm^{-3}	5581	2240	1541	836	2079 ± 410	2147 ± 189
c_V, µm^3 cm^{-3}	12854	3501	2402	762	2411 ± 537	2123 ± 202
IWC, mg m^{-3}	11.6	3.2	2.2	0.7	2.2 ± 0.5	1.91 ± 0.18

Abbreviations are particle concentration N, Junge slope k, and correlation coefficient r^2 ($n > 6$ samples) to characterize the accumulation mode aerosol; contrail particle concentration N_{cp}, mean particle diameter DM, effective diameter D_e, and ice water content IWC to characterize the contrail particle phase according to *Gayet et al.* [1996a]; additionally, mean surface concentration c_A and mean volume concentration c_V are given for the contrail particle phase (FL 310 on March 15, 1996).

* Measured with PCASP-100X.
\+ Measured with FSSP-300.

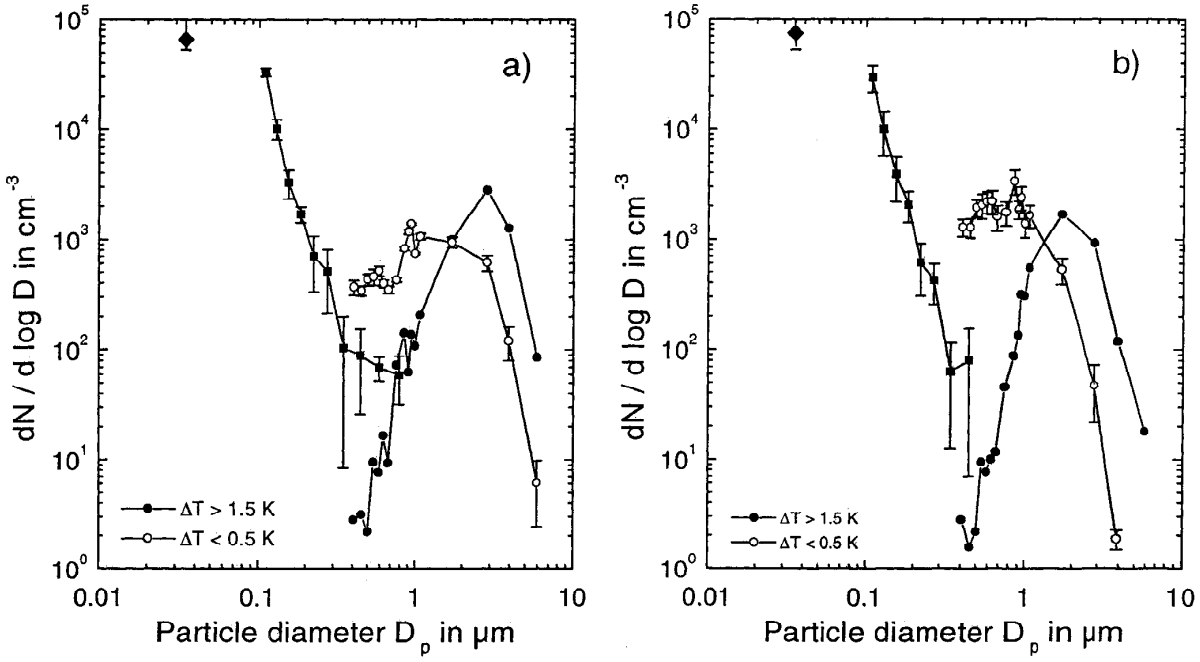

Figure 5. Size distribution of the dry accumulation mode (PCASP-100X: squares) and the contrail particles (FSSP-300: circles) inside the ATTAS contrail (FL 310 on March 15, 1996): short distance ($d \leq 250$ m, plume age < 2 s) with (a) sulfur content 6 ppm and (b) sulfur content > 2700 ppm; medium distance ($d \approx 1800$ m, plume age 10 s) with (c) sulfur content 6 ppm and (d) sulfur content > 2700 ppm; the number concentration N_{10} (diamonds) is added for completeness. The excess temperature ΔT in the near-field cases (Figures 5a and 5b) indicates whether the size distribution is measured in the plume center ($\Delta T > 1.5$ K) or at the plume edge ($\Delta T < 0.5$ K).

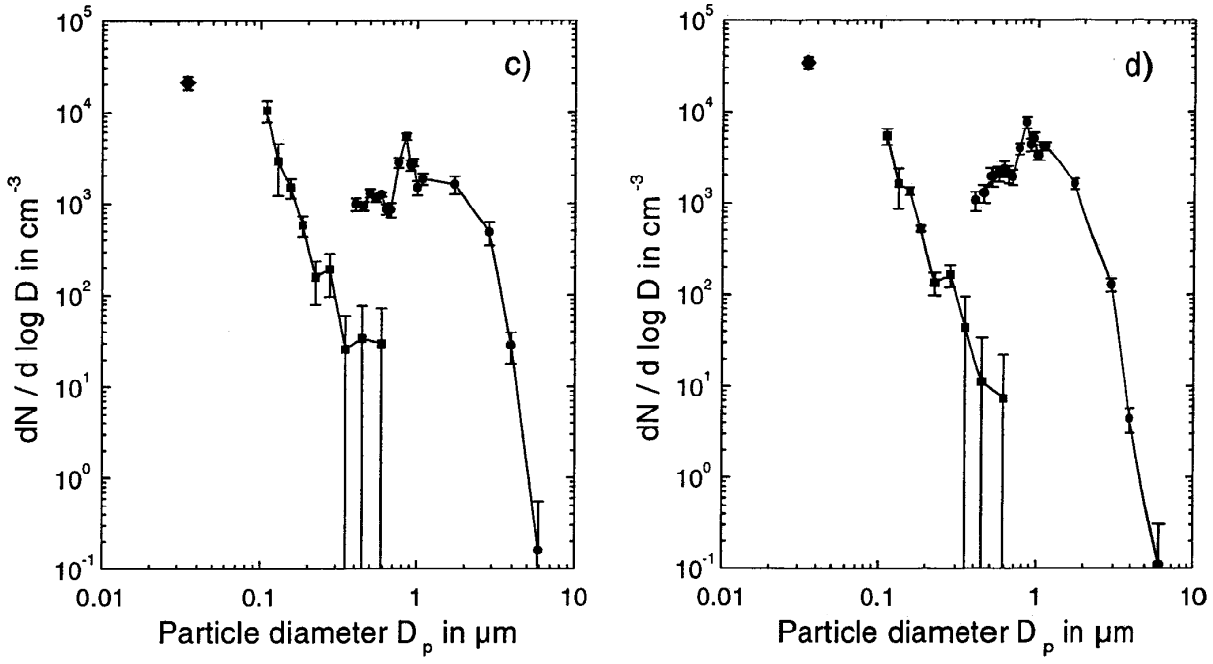

Figure 5. (continued)

3.3 Airbus A310-300 results

Measurements of the accumulation mode aerosol and contrail particles inside the Airbus A310-300 contrail are shown in Figure 6 for a flight distance $d < 400$ m (age ≤ 2.5 s). During the measurement periods, both engines burned equal fuels with fuel sulfur contents of either 850 ppm (normal) or 2700 ppm (high) at different times. No differences in contrail properties between normal sulfur and high sulfur fuel are found. This holds for both the contrail particle number concentration and size distribution. The particle number concentrations inside the contrail exceed the undisturbed background values by more than 2 orders of magnitude in both cases while the observed size range of accumulation mode particles is comparable to the ATTAS exhaust aerosol. In contrast, the contrail particles are much smaller than in the ATTAS contrail. It has to be noted that the Airbus plume reaches much higher moisture supersaturation than the ATTAS but at lower ambient humidity (see Table 2).

High sulfur measurements of the Airbus A310-300 and the ATTAS exhaust plumes are summarized in Table 6 for the short flight distance sequences. The A310-300 spectrum is enhanced over the full size range with respect to the ATTAS size distribution; the CN concentrations are again assumed to exceed 10^5 cm^{-3}. The A310-300 is emitting almost twice the amount of accumulation mode particles as the ATTAS, but it cannot be deduced whether the modern A310-300 engine (CF6-80C2A2) is causing more contrail particles than the old ATTAS engine (M45H Mk501) because of different thermodynamic conditions. Nevertheless, the ratio of accumulation mode number concentration to contrail particle number concentration is of the same order in the A310-300 plume as in the young ATTAS plume, which indicates the importance of the accumulation mode aerosol for initiating the formation of contrail particles at an age ≤ 2 s.

In Figure 7 the contrail particle size distribution is plotted at closest approach ($d \approx 100$ m, age < 1 s) of the Falcon to the leading A310-300 as measured with the standard FSSP-300 and the prototype MASP. The time resolution was 10 Hz

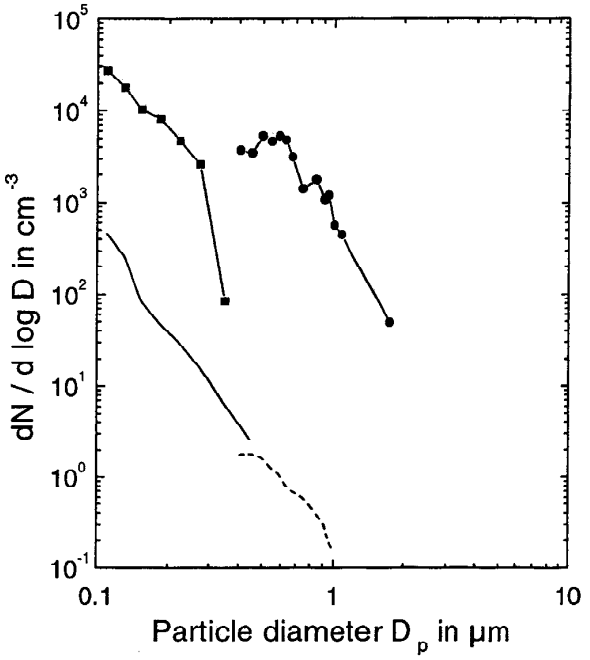

Figure 6. PCASP-100X (squares) and FSSP-300 (circles) data from measurements in the exhaust plume of an Airbus A310-300 at a flight distance $d < 400$ m (plume age ≤ 2.5 s); the background aerosol is given as solid (PCASP-100X) and dashed (FSSP-300) line, respectively.

Table 6. Particulate Phase Properties Inside the Airbus A310-300 Contrail (FL 350 on March 13, 1996) and the ATTAS Contrail (FL 310 on March 15, 1996) at a Plume Age of ≈ 2 s With High Sulfur Fuel (2700 ppm) and Respective Meteorological Conditions Added for Comparison

Parameter	A310-300	ATTAS
Ambient pressure p, hPa	238.4	287.4
Static air temperature T, K	215.0	220.7
Water vapor mixing ratio r, g kg^{-1}	< 0.03	< 0.1
Ambient relative humidity (water) RH, %	15	45
Flight distance d, m	< 400	< 300
Accumulation mode aerosol *		
N, cm^{-3}	5450	3400
Contrail particles +		
N_{cp}, cm^{-3}	1380	750
D_e, μm	0.77	2.34
IWC, mg m^{-3}	0.2	3.2

* Measured with PCASP-100X.
+ Measured with FSSP-300.

(FSSP-300) and 17 Hz (MASP). Both measured size distributions show fairly good agreement and peak at about 0.6 μm. The median diameter is almost the same as it is for larger flight distances $d < 400$ m. The differences in the spectra may result from statistical uncertainty because the spectra were measured during very short plume encounters (duration < 1 s). Also the two probes did not see the same aerosol because the plume dimension at such short flight distances is smaller than the dimensions of the measuring aircraft. Comparing these size distributions with Figure 5b, the contrail particles exhibit strong differences between the A310-300 and the ATTAS in number concentration as well as in the effective diameter. The particles are smaller in D_e by a factor of 3 compared to the ATTAS contrail, while the total number is increased by a factor of less than two. The differences in particle size and ice water content may be due to the strong differences in the meteorological conditions, especially the ambient relative humidity and maximum supersaturation inside the young plume and in different wake dynamical properties (see Tables 2 and 6). However, it also appears possible that the A310-300 exhaust aerosol itself shows a different activation behavior compared to the ATTAS exhaust aerosol because of the varying combustion conditions in the different jet engines used.

The most notable result from the IOMAS measurements during the whole flight on March 13 behind the Airbus A310-300 is that no gaseous sulfuric acid has been detected. Maximum detectable concentrations were always below the detection limit of the IOMAS, which is 5×10^7 molecules cm^{-3}, for cases both with and without visible contrail. This finding is in good agreement with model results from *Kärcher et al.* [1995], who pointed out that at distances longer than 200 m no gaseous sulfuric acid should be present inside the plume for average sulfur levels or higher. The ion measurements indicate a total aerosol surface area density of less than 6×10^3 μm^2 cm^{-3} in the A310-300 plume. A detailed description of the gaseous sulfuric acid and ion measurements is given by *F. Arnold et al.* (submitted manuscript, 1997).

4. Summary and Conclusions

The SULFUR 4 experiment yielded an extensive data set on plume and contrail properties at various ambient conditions and different fuel sulfur contents. The aircraft exhaust aerosol and contrail formation was investigated at a very short flight distance and at a medium flight distance for two different aircraft types. Data analysis focused on the measurements behind the ATTAS aircraft under contrail-forming conditions and to a minor extent on the measurements behind an Airbus A310-300 also under contrail-forming conditions but at a different flight level. The examination of the sulfur impact on the exhaust aerosol at different ambient conditions, i.e., a detailed data analysis of the ATTAS flights with and without visible contrails and at different flight levels, will be subject to further investigations.

At short flight distance ($d < 250$ m, plume age < 2 s) behind the ATTAS including the closest approach with $d = 80$ m (plume age < 1 s) the size distribution of the emitted accumulation mode aerosol exhibits the same number concentration and slope for both low and high fuel sulfur content. The CN concentration exceeds the measuring range of the CPC in all near-field plume encounters, i.e., $N_{10} > 10^5$ cm^{-3}. This was found for both dry and moist plumes, without and with visible contrail. Hence possible effects of fuel sulfur content on number concentration and ultrafine condensation nuclei fraction cannot be deduced from the closest approach measurements. As expected from theoretical predictions [*Kärcher et al.*,1995] no gaseous sulfuric acid is found inside the plume of the Airbus A310-300.

The combined in-flight measurements of static air temperature, water vapor content and contrail particle spectra

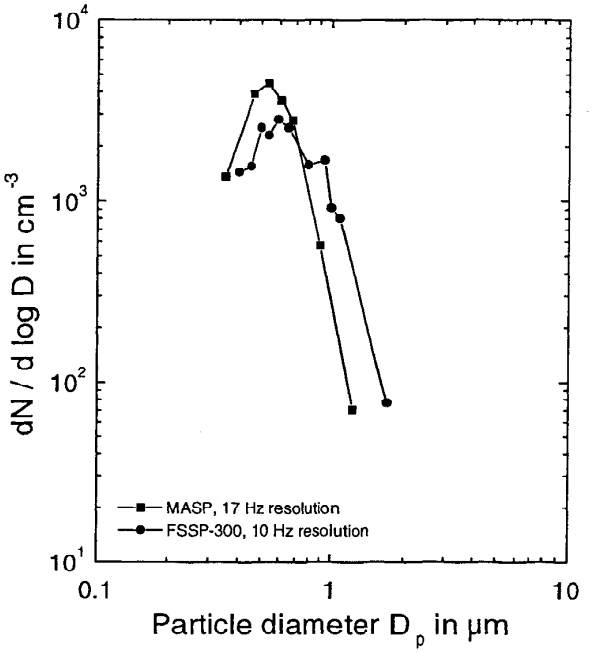

Figure 7. FSSP-300 (circles) and MASP (squares) size spectra inside the Airbus A310-300 contrail at closest approach ($d \approx 100$ m, plume age < 1 s; FL 350, $\Delta T_{max} = 2.8$ K); measured total particle number concentrations are 880 cm^{-3} (FSSP-300) and 1180 cm^{-3} (MASP).

at a very short distance behind the contrail-generating aircraft show remarkable small-scale features. For cases with visible contrail, particle size distributions exhibit strong variations from the plume center to the diluted plume edge. The respective spectra are identified by the excess temperature ΔT compared to ambient air. In the plume center $\Delta T > 1.5$ K while at the plume edge $\Delta T < 0.5$ K. In the plume center the contrail particle concentration is of comparable magnitude for both fuel sulfur contents while effective diameter and ice water content are lowered by factors 1.5 and 3.5, respectively, in the high sulfur fuel case compared to the low sulfur fuel case. These differences may be due to the strong inhomogeneity of the very young and highly turbulent plume.

At medium flight distance ($d \approx 1800$ m, plume age 10 s) the effects of fuel sulfur content on plume and contrail properties become visible. The CN concentration is enhanced by a factor of 3.5 due to a factor 500 increase in fuel sulfur content. The ultrafine condensation nuclei fraction contributes to up to 70% to the total aerosol with $D_p \geq 0.007$ μm. This UCN fraction value is of the same order of magnitude as the values reported by *Schumann et al.* [1996] for the ATTAS plume at an age of 20 s.

Major fuel sulfur induced differences occur in the in-situ aerosol phase at the plume age of ≈ 10 s. Ice water content and mean surface concentration of the contrail remain almost unaffected by the fuel sulfur. Also the small-scale variations in the contrail particle size distributions vanish at this state of contrail evolution. But the contrail particles are smaller in size and larger in number when high sulfur fuel is burned.

The overall picture of contrail formation obtained from our measurements follows theoretical predictions [*Kärcher et al.*, 1996b]. The contrail at a plume age of less than 2 s could be dominated by heterogeneous freezing of activated engine exhaust particles, which are expected to be mainly soot particles. In this first stage of contrail evolution the ratio between ice crystal concentration and accumulation mode aerosol concentration is about 0.2. The suggestion that the PCASP-measured dry accumulation mode aerosol particles are due to primary jet exhaust aerosol is confirmed by the fact that the number concentration is decreasing from > 3600 cm^{-3} (age < 2 s) to 730 - 1230 cm^{-3} (age 10 s) with increasing plume age and dilution.

After 10 s of aging the number of contrail particles is increasing by a factor of 1.7 (low sulfur fuel) to 2.7 (high sulfur fuel) compared to the plume age of < 2 s. The enhanced formation of contrail particles in the high sulfur fuel case is assumed to be caused by additional homogeneous freezing of H_2SO_4-H_2O droplets. This is conceivable when the homogeneous freezing process requires a longer timescale than heterogeneous freezing and thus cannot be observed to the full extent in the short distance measurements. At the aged state of evolution the ratio between contrail particle concentration and accumulation mode aerosol concentration has increased from 0.22 to 1.21 (low sulfur fuel) and from 0.21 to 2.73 (high sulfur fuel), respectively, compared to the young plume age. Hence, the influence of the soot particles on contrail properties seems to be restricted to the initial state of contrail development while the fuel sulfur impact becomes stronger in the aged contrail.

Comparisons of the measurements behind an Airbus A310-300 with the ATTAS measurements give evidence for an effect of the emitted primary exhaust aerosol on the properties of the young contrail (age ≤ 2 s). The Airbus plume exhibits both an increased number of exhaust aerosol particles and an increased number of contrail particles with respect to the ATTAS contrail. Part of the difference in contrail particles may be caused by different ambient conditions and wake dynamical properties. Effects of fuel sulfur content on plume and contrail properties are not observable for the Airbus A310-300 case because the fuel sulfur content was varied by a much smaller factor. Thus the interpretation of the Airbus data is restricted to an intercomparison of A310-300 and ATTAS measurements with high sulfur containing fuel. It appears possible that plume properties depend more strongly on engine type than on fuel sulfur content. We do not know how the particle properties change with power setting, but this is an important question because the ATTAS was operated at full power, while the Airbus was operated with reduced power.

A further remaining question concerns the emitted soot particle mode and its degree of activation in the exhaust plume via the uptake of H_2SO_4-H_2O droplets at short distances behind the engine exit. Related to this question the concentration of CN particles must be known more precisely to study the formation of H_2SO_4-H_2O droplets inside the plume. For this purpose the sample air which is used for the CN measurements has to be diluted in-flight with a known but variable dilution ratio. Nevertheless, the herewith presented results combined with contrail measurements at longer flight distances contribute to a better understanding of the processes near the engine exit which result in the formation of contrails.

Appendix A: Details on the Particle Measuring Instruments

The locations of the sampling inlet on the roof of the Falcon and the CPCs inside the Falcon were the same as described by *Schumann et al.* [1996] for the sulfur experiment in spring 1995. The FSSP-300 probe was mounted below the left wing at the outer position, followed by the MASP at the inner position below the left wing. The PCASP-100X probe was mounted below the right wing at the inner position (Plate 1).

The PCASP data were analyzed assuming an average refractive index of 1.58 because no detailed information was available on the chemical composition of the accumulation mode aerosol phase. Ambient number concentration values have been recalculated from post flight calibration of the pressure dependence of the instrument's volume flow rate. Uncertainties in the PCASP volume flow rate at pressure values below 500 mbar result in about 20% uncertainty for PCASP deduced aerosol number concentrations.

The FSSP-300 and MASP data were converted to size distributions of liquid water spheres (refractive index 1.33). Respective FSSP-300 channel thresholds are given by *Baumgardner et al.* [1992]. This procedure gives a negligible error in the size distribution with respect to the ice crystal phase of the cloud elements (refractive index 1.31). An unknown error is caused by the nonspherical shape of the ice crystals. It is expected to be small for young contrail particles [*Gayet et al.*, 1996b].

In order to get realistic number concentration values the CPC raw data were corrected for coincidence by multiplying them with a correction factor given by the instrument manufacturer TSI. Additionally, the N_{10} counter which was equipped with a long (3 m) and narrow (4 mm in diameter) sampling line was corrected for diffusion losses during sampling according to *Hinds* [1983]. In our data analysis we

used the factor 1.66 to correct for diffusion losses of particles with $D_p = 0.01$ μm during sampling. The N_7 and N_{18} counters were affected by diffusion losses only to a minor degree (correction factor 1.22) because they were operated with a higher flow rate (1.5 L min^{-1}) than the N_{10} counter (1 L min^{-1}) and used a wider sampling line. The particle counters were not able to resolve the very high particle number concentrations in the dense jet exhaust plume at the short measuring distance. Hence the CPC data analysis focused on the medium flight distance case. To exclude weak plume encounters with a strong fraction of entrained ambient aerosol during the determination of the UCN fraction of the total aerosol, we analyzed only peaks with $N > 2000$ cm^{-3} (see Table 4).

Appendix B: Size Distribution Analysis

The analysis of the size distribution measurements followed the procedure worked out by *Gayet et al.* [1996a]. The main parameters are contrail particle number concentration

$$N_{cp} = \sum_{i=1}^{n} N_i \quad ,$$

mean particle diameter

$$DM = \frac{\sum_{i=1}^{n} N_i D_i}{\sum_{i} N_i} \quad ,$$

effective diameter

$$D_e = \frac{\sum_{i=1}^{n} N_i D_i^3}{\sum_{i} N_i D_i^2} \quad ,$$

and ice water content

$$IWC = \frac{\pi}{6} \rho_{ice} \sum_{i=1}^{n} N_i D_i^3 \quad ,$$

with mean diameter D_i and number concentration N_i of the ith particle spectrometer channel and ice crystal density ρ_{ice} = 0.9 g cm^{-3}. All particles are assumed to be of spherical shape. Additionally, mean surface concentration c_A and mean volume concentration c_V are calculated according to *Hinds* [1983]:

$$c_A = \pi \sum_{i=1}^{n} N_i D_i^2$$

and

$$c_V = \frac{\pi}{6} \sum_{i=1}^{n} N_i D_i^3 \quad .$$

To achieve a measure for the aerosol size distribution of the dry accumulation mode, we assumed a Junge type characterized by the slope k [*Hinds*, 1983]. The slope determination was restricted to the first six channels of the PCASP which correspond to the size range $D_p < 0.3$ μm and should fit the mean mode of emitted soot particles, while the higher channels may also include larger ambient aerosol particles.

Acknowledgments. The authors are grateful to Lufthansa AG, Frankfurt, who provided the Airbus A310-300 for the measurements. The project was part of the research program "Schadstoffe in der Luftfahrt" supported by the German research ministry BMBF. The authors are grateful to many colleagues for support with the measurements and their analyses. They also wish to thank B. Kärcher from DLR for helpful discussions during the preparation of this manuscript.

References

Appleman, H., The formation of exhaust condensation trails by jet aircraft, *Bull. Am. Meteorol. Soc., 34*, 14-20, 1953.

Arnold, F., J. Scheid, Th. Stilp, H. Schlager, and M.E. Reinhardt, Measurements of jet aircraft emissions at cruise altitude I: The odd-nitrogen gases NO, NO_2, HNO_2, and HNO_3, *Geophys. Res. Lett., 19*, 2421-2424, 1992.

Baumgardner, D., J. E. Dye, and B. W. Gandrud, Interpretation of measurements made by the Forward Scattering Spectrometer Probe (FSSP-300) during the Airborne Arctic Stratospheric Expedition, *J. Geophys. Res., 97*, 8035-8046, 1992.

Baumgardner, D., and W. A. Cooper, Airborne measurements in jet contrails: Characterization of the microphysical properties of aircraft wakes and exhausts, *DLR-Mitt. 94-06*, pp. 418-423, Dtsch. Zentrum für Luft- und Raumfahrt, Köln, Germany, 1994.

Baumgardner, D., J. E. Dye, B. Gandrud, K. Barr, K. Kelly, and K. R. Chan, Refractive indices of aerosols in the upper troposphere and lower stratosphere, *Geophys. Res. Lett., 23*, 749-752, 1996.

Brown, R. C., R. C. Miake-Lye, M. R. Anderson, C. E. Kolb and T. J. Resch, Aerosol dynamics in near-field aircraft plumes, *J. Geophys, Res., 101*, 22,939-22,953, 1996a.

Brown, R. C., M. R. Anderson, R. C. Miake-Lye, C. E. Kolb, A. A. Sorokin, and Y. Y. Buriko, Aircraft exhaust sulfur emissions, *Geophys. Res. Lett., 23*, 3603-3606, 1996b.

Busen, R., and U. Schumann, Visible contrail formation from fuels with different sulfur contents, *Geophys. Res. Lett., 22*, 1357-1360, 1995.

Busen, R., D. Baumgardner, S. Borrmann, D. E. Hagen, M. Kuhn, A. Petzold, F. P. Schröder, U. Schumann, J. Ström and P. D. Whitefield, Experiments on contrail formation from fuels with different sulfur content, in *Proceedings of the International Colloquium on the Impact of Aircraft Emissions Upon the Atmosphere*, Vol. I, pp. 149-154, Off. Nat. d'Etudes et de Rech. Aeros., Chatillon, France, 1996.

Fahey, D. W. *et al.*, Emission measurements of the Concorde supersonic aircraft in the lower stratosphere, *Science, 270*, 70-74, 1995a.

Fahey, D. W. *et al.*, In situ observations in aircraft exhaust plumes in the lower stratosphere at midlatitudes, *J. Geophys. Res., 100*, 3065-3074, 1995b.

Farago, Z., Fuel sulfur content, sulfur-oxide emissions, and corrosion in oil heating plants, *Combust. Sci. Technol., 79*, 73-96, 1991.

Frenzel, A., and F. Arnold, Sulfuric acid cluster ion formation by jet engines: Implications for sulfuric acid formation and nucleation, *DLR-Mitt. 94-06*, pp. 106-112, Dtsch. Zentrum für Luft- und Raumfahrt, Köln, Germany, 1994.

Gayet, J.-F., G. Febvre, G. Brogniez, H. Chepfer, W. Renger, and P. Wendling, Microphysical and optical properties of cirrus and contrails: Cloud field study on 13 October 1989, *J. Atmos. Sci., 53*, 126-138, 1996a.

Gayet, J.-F., G. Febvre, and H. Larsen, The reliability of the PMS FSSP in the presence of small ice crystals, *J. Atmos. Oceanic Technol., 13*, 1300-1310, 1996b.

Gerz, T., and T. Ehret, Wingtip vortices and exhaust jets during the jet regime of aircraft wakes, *Aerospace Sci. Techn*, in press, 1997.

Gierens, K., and U. Schumann, Colors of contrails from fuels with different sulfur contents, *J. Geophys. Res., 101*, 16,731-16,736, 1996.

Hagen, D. E., P. D. Whitefield, and H. Schlager, Particle emissions in the exhaust plume from commercial jet aircraft under cruise conditions, *J. Geophys. Res., 101*, 19,551-19,557, 1996.

Hinds, W.C., *Aerosol Technology*, John Wiley, New York, 1983.

Hofmann, D. J., and J. M. Rosen, Balloon observations of a particle layer injected by stratospheric aircraft at 23 km, *Geophys. Res. Lett., 5*, 511-514, 1978.

Kärcher, B., Aircraft-generated aerosols and visible contrails, *Geophys. Res. Lett., 23*, 1933-1936, 1996.

Kärcher, B., Th. Peter, and R. Ottmann, Contrail formation: Homogeneous nucleation of H_2SO_4-H_2O droplets, *Geophys. Res. Lett.*, *22*, 1501-1504, 1995.

Kärcher, B., M. M. Hirschberg, and P. Fabian, Small-scale chemical evolution of aircraft exhaust species at cruising altitudes, *J. Geophys. Res.*, *101*, 15,169-15,190, 1996a.

Kärcher, B., Th. Peter, U. M. Biermann, and U. Schumann, The initial composition of jet condensation trails, *J. Atmos. Sci.*, *53*, 3066-3083, 1996b.

Knollenberg, R. G., Measurements of the growth of the ice budget in a persisting contrail, *J. Atmos. Sci.*, *29*, 1367-1374, 1972.

Miake-Lye, R. C., R. C. Brown, M. R. Anderson and C. E. Kolb, Calculations of condensation and chemistry in an aircraft contrail, *DLR-Mitt. 94-06*, pp. 274-279, Dtsch. Zentrum für Luft- und Raumfahrt, Köln, Germany, 1994.

Petzold, A., and F. P. Schröder, Jet engine exhaust aerosol characterization, *Aerosol Sci. Technol.*, in press, 1997.

Petzold. A., J. Ström, S. Ohlsson, and F. P. Schröder, Elemental composition and morphology of ice crystal residual particles in cirrus clouds and contrails, *Atmos. Res.*, accepted, 1997.

Pitchford, M., J. G. Hudson, and J. Hallet, Size and critical supersaturation for condensation of jet engine exhaust particles, *J. Geophys. Res.*, *96*, 20,787-20,793, 1991.

Ponater, M., S. Brinkop, R. Sausen, and U. Schumann, Simulating the global atmospheric response to aircraft water vapor emissions and contrails - A first approach using a GCM, *Ann. Geophys.*, *14*, 941-960, 1996.

Schmidt, E., Die Entstehung von Eisnebel aus den Auspuffgasen von Flugmotoren, *Schr. Dtsch. Akad. Luftfahrtforschung*, *44*, 1-22, 1941.

Schröder F. P., and J. Ström, Aircraft measurements of submicrometer aerosol (> 7 nm) in the upper troposphere and tropopause region, *Atmos. Res.*, *44*, 333-356, 1997.

Schumann, U., On the effect of emissions from aircraft engines on the state of the atmosphere, *Ann. Geophys.*, *12*, 365-384, 1994.

Schumann, U., On conditions for contrail formation from aircraft exhausts, *Meteorol. Z.*, *NF 5*, 4-23, 1996a.

Schumann, U., Particle formation in jet aircraft exhausts and contrails for different sulfur containing fuels, in *Nucleation and Atmospheric Aerosols*, edited by M. Kulmala and P.E. Wagner, pp. 296-299, Pergamon, Oxford, UK ,1996b.

Schumann, U., J. Ström, R. Busen, R. Baumann, K. Gierens, M. Krautstrunk, F. P. Schröder, and J. Stingl, In situ observations of particles in jet aircraft exhausts and contrails for different sulfur-containing fuels, *J. Geophys. Res.*, *101*, 6853-6869, 1996.

Strapp, J. W., W. R. Leaitch, and P. S. K. Liu, Hydrated and dried aerosol-size-distribution measurements from the particle measuring systems FSSP-300 probe and the deiced PCASP-100X probe, *J. Atmos. Oceanic Technol.*, *9*, 548-555, 1992.

Ström, J., In-situ observations of interstitial aerosol particles and cloud residues found in contrails, in *Proceedings of the International Colloquium on the Impact of Aircraft Emissions Upon the Atmosphere*, Vol. I, pp. 445-448, Off. Nat. d'Etudes et de Rech. Aeros., Chatillon, France, 1996.

Zhao, J., and R. P. Turco, Nucleation simulations in the wake of a jet aircraft in stratospheric flight, *J. Aerosol Sci.*, *26*, 779-795, 1995.

F. Arnold, Atmospheric Physics Division, Max-Planck-Institut für Kernphysik, D-69127 Heidelberg, Germany.

R. Baumann, R. Busen, M. Kuhn, A. Petzold, F. P. Schröder, U Schumann, Institut für Physik der Atmosphäre, DLR Oberpfaffenhofen, D-82234 Wessling, Germany (e-mail: andreas.petzold@dlr.de)

D. Baumgardner, Research Aircraft Facility, National Center for Atmospheric Research, Boulder, CO 80307.

S. Borrmann, Institut für Physik der Atmosphäre, Universität Mainz, D-55099 Mainz, Germany.

D. E. Hagen and P. D. Whitefield, Cloud and Aerosol Sciences Laboratory, University of Missouri at Rolla, Rolla, MO 65401-0249.

J. Ström, Stockholms Universitet, Meteorologiska Institutionen, S-10691 Stockholm, Sweden.

(Received March 14, 1997; revised July 22, 1997;
accepted August 1, 1997.)